

Development of isolation system for ambient micro-vibration and earthquake using multi-stage rubber bearings and high damping rubber damper

H. Yanbe
Graduate School of Tokyo Denki University, Japan

S. Fujita
Tokyo Denki University, Japan

N. Masaki & M. Ohta
Bridgestone Corporation, Japan

ABSTRACT: In industrial facilities such as semiconductor manufacturing factories, it is desirable to have isolation floor which are effective not only for strong earthquakes but also for weak earthquakes and even for ambient micro-vibration. As a first step of research, a two-dimensional isolation floor was developed to satisfy such requirements. The results show that the isolation floor using multi-stage rubber bearings and high damping rubber damper is able to reduce the acceleration of the floor to 1/2~2/3 of the floor slab. And the analytical results considering displacement dependent stiffness and linear viscous damping characteristic of the damper agree well with the experimental results.

1 INTRODUCTION

In recent years, Japanese manufacturing, construction and engineering industries, have paid a great deal of attention to the development of technology capable of isolating ambient micro-vibrations (Fujita, T. 1987: No. 496, Fujita, T. 1990: No. 521, Fujita, T. 1987: No. 490). The most demanding of these developers is the semiconductor industry, where deterioration in stability has a major impact on yield ration and can ruin the accuracy of the industry's ultra-precise machining processes. Currently, the most popular method used to isolate these processes from micro-vibrations is the construction of an isolation floor supported by pneumatic shock absorbers, springs and other methods. In addition to passive isolation active methodology has also been extensively researched (Fujita, T. 1990: No. 523). However, most current vibration isolation equipment only attenuates vibration frequencies below 50 Hz. It should also be remembered that advancements in super LSI technology have made development of ultra-precision measurement technology imperative. Parallel to demands in that area is the urgent need for a way to isolate vibration with an acceleration of 10^{-4} gal ($= \text{cm/s}^2$) and a displacement in the sub nanometer ($\text{nm} = 10^{-6} \text{ mm}$) level. This paper describes the application of the authors' new high damping rubber damper to vibration isolation equipment incorporating a multi-stage rubber bearing and explains the system's effectiveness against constant micro-vibration.

2 EXPERIMENTAL SYSTEM

Figure 1 and 2 shows the vibration isolation system used for the experiment. In this experiment, a vibration floor measuring $2,000 \text{ mm} \times 1,500 \text{ mm} \times 312^H \text{ mm}$ and with a mass of $4,000 \text{ kg}$ is supported by four multi-stage rubber bearings, as seen in Fig. 1. Each multi-stage rubber bearing is designed with natural frequencies of 0.57 Hz in its horizontal direction and 17 Hz in its vertical direction when acted upon by a $1,000 \text{ kg}$ mass.

The natural vertical frequency indicates the bearings do not isolate vertical vibration and/or earthquakes as efficiently as they protect against horizontal vibration.

Figure 3 shows the high damping rubber damper used for this test. It features a unique, relatively soft, highly malleable, rubber material measuring $50 \text{ mm} \times 50 \text{ mm} \times 10^T \text{ mm}$ which is sandwiched between steel plates. Damping force is generated by material distortion resulting from horizontal shear stress acting on the multi-stage rubber bearings.

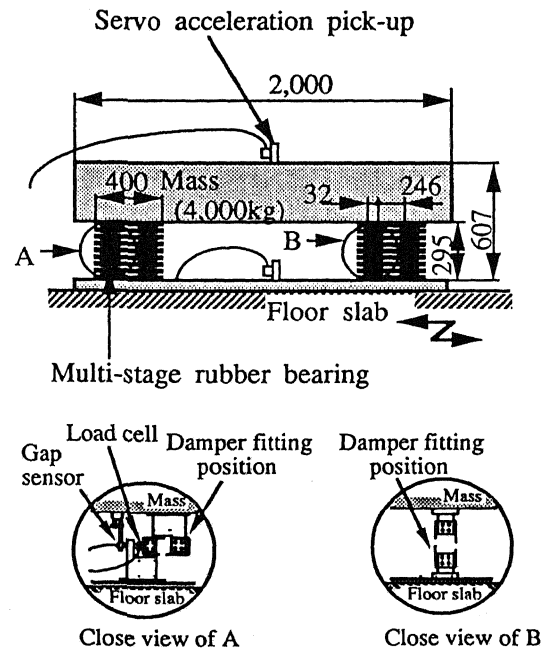


Fig.1 Schematic View of Isolation System and Measurement Points

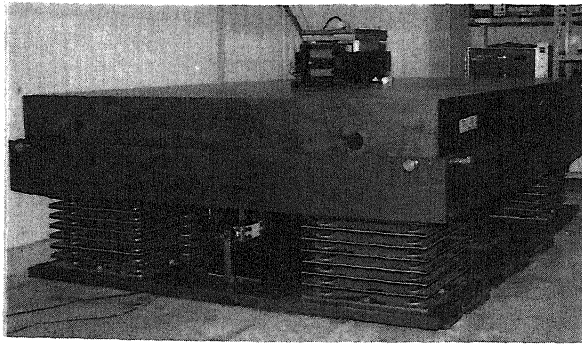


Fig.2 Isolation System for Ambient Micro-Vibration and Earthquake Using Multi-Stage Rubber Bearings and High Damping Rubber Damper

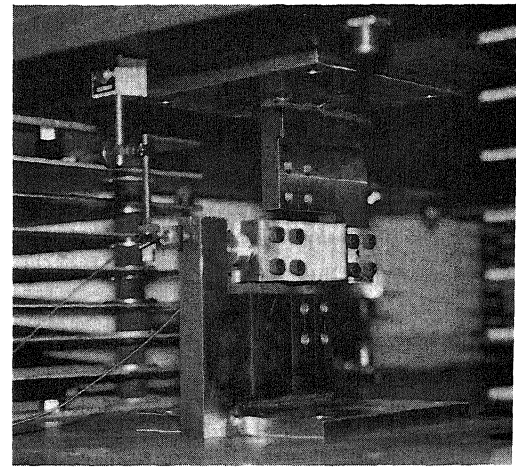


Fig.4 High Damping Rubber Damper Installed in the System

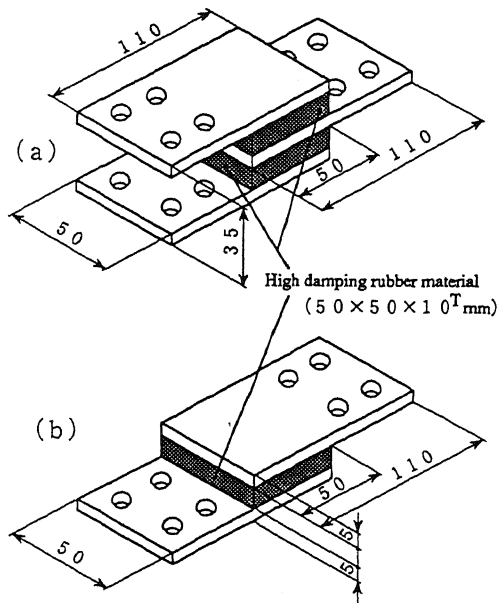


Fig.3 High Damping Rubber Damper Used for The Test

3 EXPERIMENT

3.1 Test on high damping rubber damper

The shear modulus (represented by G) and the loss factor (represented by $\tan\delta$) were calculated based on the restoring characteristic measurements of the rubber material incorporated into the damper. The Static Excitation experiment was conducted using a single-axis actuator in the strain region between one and 100 percent. In the lower strain region -- between 0.02 and 2 percent -- restoring characteristics of the high damping rubber were achieved by applying forced displacement amplitude. In this experiment, the excitor was installed on the system (see Fig. 2) with the damper shown in Fig. 3 (a) attached to the portion symbolized by A (see Fig. 4). A 1 Hz sine wave was used as the excitation force for the system in both cases.

3.2 Constant micro-vibration input experiment

The constant micro-vibration isolating effectiveness was measured with two dampers (see Fig. 3 (a)) installed at the areas A and B in Fig. 1. Floor slab and system accelerations were measured by a servo acceleration pick-up. A non-contact displacement gauge was utilized to measure the relative displacement between the isolation floor and the floor slab. The force acting on the dampers were measured using a load cell.

4 ANALYTICAL MODEL

Figure 5 depicts the analytical model which allows for two degrees of freedom in its swaying and rocking motions. Equations (1) and (2) listed below define the horizontal and vertical strain characteristics of the multi-stage rubber bearing. Equation (3) specifies both of the horizontal and the vertical damping characteristics of the high damping rubber damper. The damper's horizontal and vertical damping coefficients are defined by Eq. (4).

$$K_{TH} = 6.00 \times 10^4 \text{ N/m} \quad (1)$$

$$K_{TV} = 3.55 \times 10^7 \text{ N/m} \quad (2)$$

$$K_{DH} = K_{DV} = K_0 \{ 1.33 \exp(-4.3 \times 10^2 |x|) + 1.0 \} \text{ N/m} \quad (3)$$

$$C_{DH} = C_{DV} = \alpha K_0 \text{ Ns/m} \quad (4)$$

$$K_0 = 1.50 \times 10^5 \text{ N/m} \quad (5)$$

The damper deformation amount is represented by x . α is a proportional constant. It should be noted that damping was regarded as linear viscous in this research. This is because the characteristics of the damper used here are very similar to that of linear viscous damping (Fujita, S 1991).

5 RESULTS OF EXPERIMENT AND ANALYSIS

5.1 High damping rubber damper characteristics

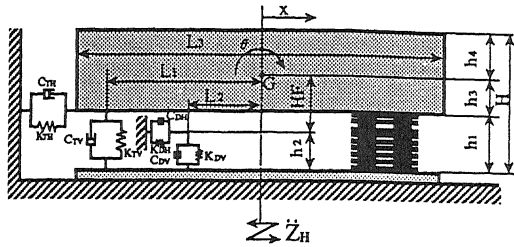


Fig.5 Analytical model

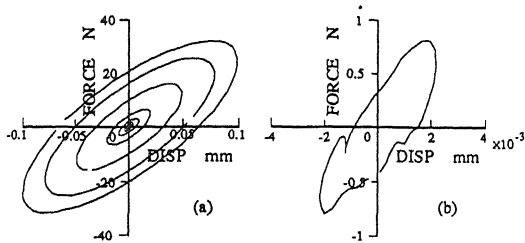


Fig.6 Restoring Force Characteristics of High Damping Rubber Damper

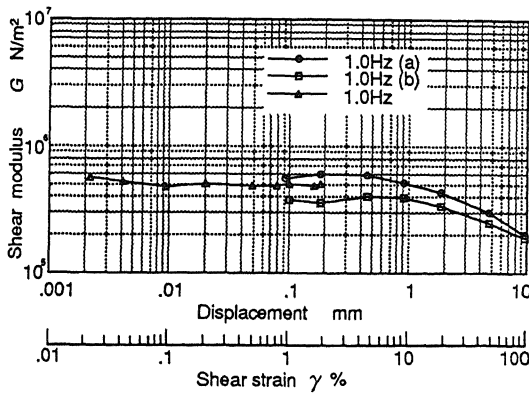


Fig.7 Shear Modulus vs Shear Strain

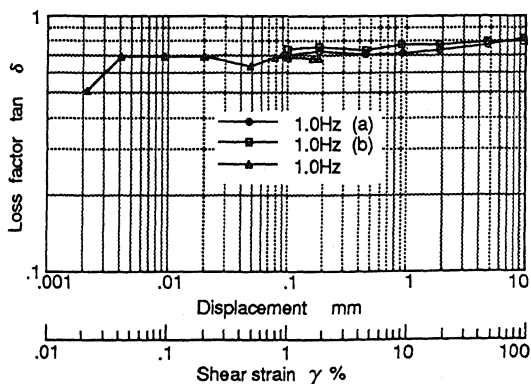


Fig.8 Loss Factor vs Shear Strain

Figure 6 (a) shows the restoring force characteristics of the damper under the amplitude between two and 100 μm ; while Figure 6 (b) shows those under the amplitude of 2 μm . As a result, we confirmed that this damper was capable of effectively absorbing unfavorable energy even when vibration input was kept extremely low. The damper also shows an effective hysteresis loop when graphed.

Figure 7 reveals the dependence of shearing modulus G upon shearing strain. Figure 8 shows dependence of loss factor ($\tan\delta$) upon shearing strain. In the large displacement region where such strain diminishes, G tends to increase while \tan shows a moderate decreasing tendency. Under 100 μm , however, they both remain close to constant. In these figures a line (a) shows the results achieved by applying gradually-increasing strain amplitude to a new damper. A line (b) shows the result achieved immediately after the measurement for a line (a). These experiments proved that small amplitude stiffness decreased after large damper deformation occurrences.

5.2 Vibration isolation characteristics

Figure 9 provides the time history responses for ambient micro-vibrations and shows acceleration input, responsive acceleration and displacement. The data includes vibration components up to 500 Hz. The response to acceleration input in each case was reduced by approximately 15 percent without the damper compared to an approximate 57 percent reduction with the damper installed. One unfavorable condition in our experiment was that the floor slab of the vibration isolation system was not a true building foundation -- thus interjecting a variable in floor slab acceleration calculations obtained from damper installation on the system. However, one separate report (Fujita, S. 1987) revealed that a system featuring isolation performance similar to our system was capable of reducing responsive acceleration by approximately 12.5 percent without a damper. Consequently, more favorable performance can be expected if installation conditions are better.

Figure 10 shows the frequency transfer function achieved by smoothing the power spectra of the input and the responsive accelerations using a 8,192-point Hanning window. In situations without a damper, the first-order natural frequency reached its peak at 0.61 Hz while the second-order rocking mode peaked at around 25 Hz. When comparing the cases with and without dampers, responsive accelerating occurring at specified frequencies were reduced by the damper. The first-order natural frequency, however, tends to vary widely according to further optimize damper capacity. Furthermore, it was proven that the damper failed to effectively reduce the responsive acceleration occurring in the several hundred Hz region.

Figure 11 provides the results of the analysis performed using the two-degree-of-freedom model, to which acceleration measured at the floor slab was applied. The value of the acceleration was achieved in

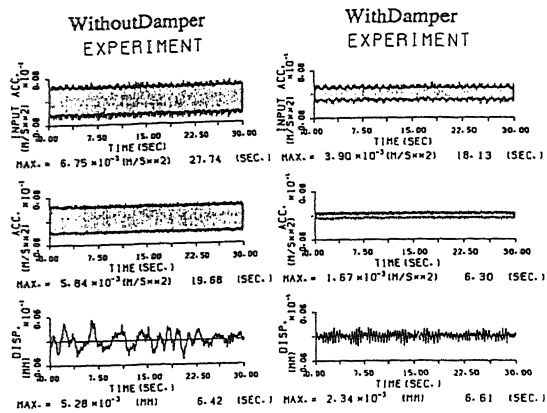


Fig.9 Performance of isolation for Ambient Micro-Vibration

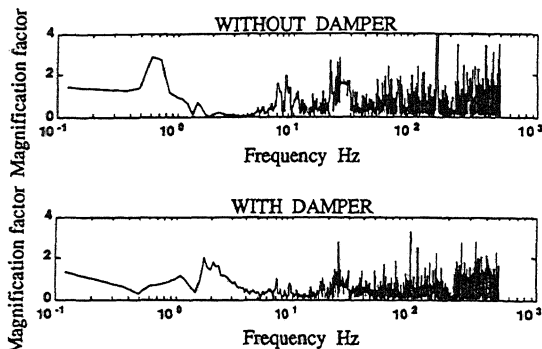


Fig.10 Transfer Function

the micro-vibration experiment described above. The analytical result of the relative displacement conformed well to the experimental result shown in Fig. 9. However, these did not agree with each other in terms of resonance acceleration. This shows the two-degree-of-freedom model falls short of correctly achieving responsive acceleration.

6 CONCLUSION

The following results were achieved by the basic experiments conducted using the high damping rubber damper and other experiments conducted by applying the damper to the multi-stage rubber bearing system:

- (1) It was confirmed that the newly-developed high damping rubber damper showed favorable energy absorbing performance in the micro strain amplitude region.
- (2) The analytical responsive displacement agreed with the experiment results. This was confirmed by a simulation conducted to determine the damper's basic characteristics. The two-degree-of-freedom model was used for the simulation.
- (3) Although the isolation floor used in this study was capable of reducing vibration under 50 Hz, it was incapable of attenuating those frequencies in the several hundred Hz range.

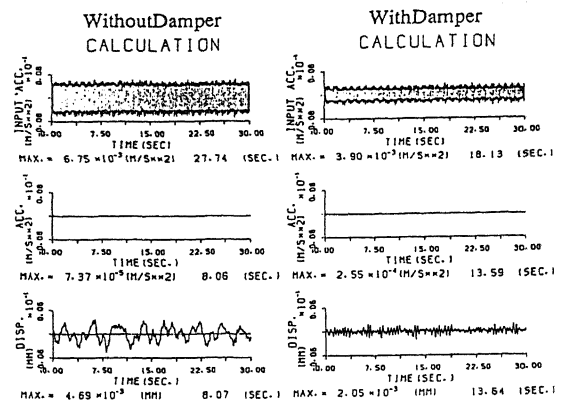


Fig.11 Results of Theoretical analysis

The next step of our research will focus on the high frequency component of the micro-vibration and development of vibration isolation technology that will upgrade performance in that region .

ACKNOWLEDGEMENTS

The authors would like to express their appreciation to the following graduates of Tokyo Denki University, Mr. K. Watanabe and Mr. K. Ochiwa, for their great assistances.

REFERENCES

- Fujita, T., et al. 1987: *A three-dimensional isolation floor for earthquake and ambient micro-vibration using multi-stage rubber bearings (1st report)*. *Trans. Jpn. Soc. Mech. Eng. Vol. 53, No. 496, C: 2521-2527*
- Fujita, T., et al. 1990: *A three-dimensional isolation floor for earthquake and ambient micro-vibration using multi-stage rubber bearings (2nd report)*. *Trans. Jpn. Soc. Mech. Eng. Vol. 56, No. 521, C: 43-48*
- Fujita, T., et al. 1987: *Experimental study of multi-stage rubber bearings developed for an isolation floor for earthquakes and ambient micro-vibration*. *Trans. Jpn. Soc. Mech. Eng. Vol. 53, No. 490, C: 1147-1152*
- Fujita, T., et al. 1990: *Active microtremor isolation system using linear motors*. *Trans. Jpn. Soc. Mech. Eng. Vol. 56, No. 523, C: 628-633*
- Fujita, S., et al. 1991: *Seismic response of steel framed buildings using viscoelastic damper*. *Trans. 11th SMIRT. Vol. K2: 109-114*